Acta Cryst. (1976). B32, 254

The Structure of Methyl (4*R*)-2β-Bromo-3-oxo-19-nor-16α-(−)-kauran-17-oate, $C_{20}H_{29}O_3Br$*

By Ivan F. Taylor Jr and William H. Watson

FASTBIOS Laboratory, Texas Christian University, Fort Worth, Texas 76129, *U.S.A.*

(*Received* 24 *April* 1975; *accepted* 19 *May* 1975)

The structure of methyl (4*R*)-2β-bromo-3-oxo-19-nor-16α-(−)-kauran-17-oate, $C_{20}H_{29}O_3Br$, was determined by application of Patterson and Fourier techniques. The material crystallizes in space group $P2_12_12_1$ with cell dimensions $a=7{\cdot}71(1)$, $b=31{\cdot}77(1)$ and $c=7{\cdot}72(1)$ Å with $Z=4$. The crystals decompose rapidly upon exposure to X-rays and slowly upon exposure to the atmosphere. Counter techniques were used to collect 1112 intensities of which 570 were greater than $3\sigma(I)$. The structure was refined by least-squares techniques to a final *R* of 0·083. The molecule exhibits the kaurane skeleton with *trans*-fused *A* and *B* rings and *cis*-fused *B* and *C* rings. The six-membered rings are in the chair conformation with distortion increasing from the *A* to the *C* ring due to bridging across the *C* ring.

Introduction

Kaurene-type diterpenoids have been isolated from a number of plant species and many of them are of interest because of their gibberellin-like activity (Hanson, 1968; Goodwin, 1971). The structures of two related compounds, (−)-kaur-15-en-19-al (I) (Karle, 1972) and 7β-hydroxykaurenolide (II) (Hanson, McLaughlin & Sim, 1972), have been reported. Because of our interest in the structures of biologically active natural products, a sample of methyl (4*R*)-2β-bromo-3-oxo-19-nor-16α-(−)-kauran-17-oate (III) was submitted to our laboratory by Dr K. Venkatasubramanian.

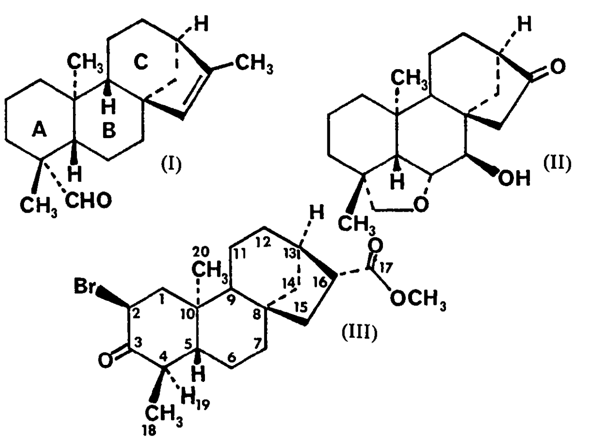

Experimental

The crystals were prismatic with the long axis coincident with the crystallographic *c* axis. The crystals were mounted along the *b* axis to insure peak resolution on the Pailred diffractometer. Room-temperature lattice parameters were obtained by a least-squares analysis of data from precession photographs calibrated with reflections from a single crystal of sodium chloride. Owing to a lack of sample, an accurate density was not determined.

Crystal data

$C_{20}H_{29}O_3Br$, M.W. 397·36. $a=7{\cdot}71$ (1), $b=31{\cdot}77$ (1), $c=7{\cdot}72$ (1) Å. Space group: $P2_12_12_1$ (No. 19). $Z=4$, $F(000)=832$, $V=1891{\cdot}7$ Å^3, $\mu=33{\cdot}8$ cm^{-1}, $D_{exp}=1{\cdot}3$, $D_{cal}=1{\cdot}395$ g cm^{-3}.

A crystal of dimensions 0·40 × 0·20 × 0·45 mm was mounted with the *b* axis coincident with the rotation axis. Intensity data, *h*0*l* through *h*22*l*, were collected with a Philips Pailred diffractometer using equi-inclination geometry, the continuous ω-scan technique, Cu *Kα* radiation (λ = 1·54178 Å) and a graphite monochromator. Scan widths ranged from 5 to 7° with the scan speed fixed at 2·5° min^{-1}. A 10s background count was taken on either side of the scan range. 1112 independent reflections were measured and 570 had intensities greater than $3\sigma(I)$. The intensities of the standard reflections decreased by 50% during data collection and the intensity data were corrected graphically. The data were corrected for Lorentz–polarization factors and absorption and were adjusted to an absolute scale by a Wilson plot. Standard deviations were assigned initially on the basis of counting statistics; however, owing to the poor quality of the data, an empirical weighting scheme was used during final refinement. Scattering factors of Cromer & Waber (1965) were used for Br, C and O, while those of Stewart, Davidson & Simpson (1965) were used for H. The scattering factor for Br was corrected for the real and imaginary parts of the anomalous dispersion.

Structure determination and refinement

A three-dimensional sharpened Patterson map provided the coordinates for the Br atom in the bromo-

* Contribution No. 18 from the FASTBIOS Laboratory.

kaurane structure. Phases based on the Br coordinates were used to calculate an electron density map which revealed the location of the cyclohexanone fragment adjacent to the Br atom. The small quantity of poor data led to repeated structure factor calculations and analyses of Fourier maps before the remaining atoms were located. The small data set produced series termination errors which were clearly visible in electron density maps as ripples radiating from the bromine atom. Full-matrix least-squares refinement of the positional parameters of all non-H atoms brought the discrepancy index to 0·095 where $R=[\sum||F_o|-|F_c||/\sum|F_o|]$. The Br atom was refined anisotropically. A plot of ΔF *vs* F gave a line of small curvature which could be fitted by a straight line with zero slope, and a unit weighting scheme was adopted. Positions of all ring H atoms were calculated on the assumption of a tetrahedral geometry. After the ring H atom parameters were included in a structure factor calculation, peaks consistent with methyl H atom positions for C(18) and C(20) were observed in the difference map. Positional and thermal parameters of the ring and methyl H atoms were included in the final cycles of least-squares but were not refined. Refinement using 570 reflections was terminated with $R=0·083$ and $R_w=0·090$ where $R_w=[\sum w(|F_o|-|F_c|)^2/(\sum w|F_o|)^2]^{1/2}$.

The function minimized was $\sum w(|F_o|-|F_c|)^2$ where $w=1$. A final three-dimensional Fourier map contained a number of positive areas, but none corresponded to possible structural features. The estimated standard deviations were calculated from the inverse of the normal-equations matrix of the last least-squares cycle. The standard deviations in C–C bond lengths is about 0·03 Å and in bond angles about 2°. All shifts of the parameters during the final cycles were less than 0·05 of the estimated standard deviation. The atomic and thermal parameters along with the estimated standard deviations are given in Table 1.*

Table 1. *Positional and isotropic thermal parameters*

	x	y	z	B
C(1)	2243 (32)	1081 (10)	8920 (32)	3·6 (6)
C(2)	1713 (43)	707 (12)	9837 (40)	6·4 (8)
C(3)	3170 (37)	480 (10)	10608 (36)	4·0 (7)
C(4)	4590 (34)	345 (10)	9321 (31)	4·0 (7)
C(5)	5113 (48)	765 (9)	8527 (31)	4·7 (5)
C(6)	6742 (50)	732 (14)	7480 (45)	8·4 (11)
C(7)	7407 (41)	1165 (12)	6892 (42)	6·2 (8)
C(8)	6085 (34)	1444 (9)	5841 (32)	3·2 (6)
C(9)	4377 (30)	1411 (9)	6943 (32)	3·5 (6)
C(10)	3656 (35)	1005 (10)	7552 (33)	3·7 (6)
C(11)	2996 (51)	1676 (13)	5945 (46)	7·3 (10)
C(12)	3072 (51)	1653 (12)	4074 (45)	7·6 (10)
C(13)	4866 (50)	1674 (10)	3294 (34)	5·4 (6)
C(14)	5804 (36)	1320 (11)	4043 (34)	4·6 (7)
C(15)	6745 (41)	1859 (11)	5598 (40)	5·5 (8)
C(16)	5970 (41)	2076 (12)	3958 (41)	6·7 (9)
C(17)	7307 (51)	2166 (14)	2529 (49)	7·4 (10)
C(18)	6072 (42)	73 (10)	10175 (38)	5·7 (8)
C(20)	2871 (32)	724 (10)	6115 (29)	3·7 (6)
C(21)	7728 (74)	2539 (18)	34 (78)	11·3 (12)
O(22)	8755 (38)	2134 (9)	2696 (35)	9·6 (8)
O(23)	6442 (33)	2411 (8)	1422 (33)	8·7 (7)
O(24)	3304 (28)	339 (7)	12058 (28)	7·0 (6)
Br	−42 (7)	819 (2)	11606 (5)	*
H(1)	2644	1296	9733	5·0
H(1′)	1213	1208	8362	5·0
H(2)	1086	520	9070	5·0
H(4)	4111	170	8463	5·0
H(5)	5322	980	9431	5·0
H(6)	7644	581	8067	5·0
H(6′)	6484	565	6400	5·0
H(7)	8496	1132	6216	5·0
H(7′)	7811	1321	7903	5·0
H(9)	4434	1610	7892	5·0
H(11)	3115	1978	6317	5·0
H(11′)	1839	1610	6379	5·0
H(12)	2466	1396	3717	5·0
H(12′)	2328	1877	3589	5·0
H(13)	4772	1687	2042	5·0
H(14)	6921	1294	3466	5·0
H(14′)	5097	1071	4009	5·0
H(15)	7991	1859	5499	5·0
H(15′)	6457	2032	6612	5·0
H(16)	5184	2317	4115	5·0
H(18)	3250	4850	5714	5·0
H(18′)	4200	5580	4762	5·0
H(18″)	5000	4780	3333	5·0
H(20)	7000	4480	3333	5·0
H(20′)	6950	3920	4762	5·0
H(20″)	9000	4500	4762	5·0

* Anisotropic temperature parameters for Br × 10^3. $U_{11}=75$ (2), $U_{22}=197$ (5), $U_{33}=73$ (2), $U_{12}=-33$ (4), $U_{13}=22$ (3), $U_{23}=-13$ (4).

Discussion

Fig. 1 shows a projection of the unit-cell contents onto the *ab* plane while Fig. 2 gives the structure of a single kaurane molecule and indicates the numbering scheme used in all tables. Table 2 lists bond distances, bond angles and torsion angles.

The molecules are packed loosely with O(23)–C(21) = 3·08 Å and O(24)–C(20) = 3·40 Å being the shortest intermolecular contacts. Four other interactions lie between 3·4 and 3·6 Å. No interaction in the (−)-kaur-15-en-19-al (Karle, 1972) structure is less than 3·7 Å. The three six-membered rings have chair conformations with the *A–B* rings *trans* fused and the *B–C* rings *cis* fused. The internal torsion angles around the three six-membered rings are similar to those reported for (−)-kaur-15-en-19-al (Karle, 1972), but the torsion angles in the five-membered ring differ significantly owing to the absence of the C(14)–C(15) double bond. The five-membered ring has the envelope conformation. The torsion angles around ring *A* are close to the ideal value of 60°, but the distortion increases from the *A* to the *C* ring due to the bridging five-membered ring. The conformation and torsion angles differ considerably from those reported in 7β-hydroxykaurenolide (Hanson, McLaughlin & Sim, 1972) which has a γ-lactone function bridging the *A* and *B* rings. A model

* A list of structure factors has been deposited with the British Library Lending Division as Supplementary Publication No. SUP 31137 (4 pp.). Copies may be obtained through The Executive Secretary, International Union of Crystallography, 13 White Friars, Chester CH1 1NZ, England.

of the kaurane molecule utilizing idealized bond angles shows a strong intramolecular interaction between the C(20) methyl group and ring carbons C(12) and C(14);

Table 2. *Bond distances* (Å) *and angles* (°)

Bond distances

C(1)—C(2)	1·44	C(8)—C(9)	1·57	C(13)-C(16)	1·62
C(2)—C(3)	1·46	C(9)—C(10)	1·48	C(16)-C(17)	1·54
C(3)—C(4)	1·54	C(9)—C(11)	1·56	C(4)—C(18)	1·58
C(4)—C(5)	1·52	C(11)-C(12)	1·45	C(10)-C(20)	1·55
C(5)—C(10)	1·55	C(12)-C(13)	1·51	C(17)-O(22)	1·33
C(10)-C(1)	1·54	C(13)-C(14)	1·46	C(17)-O(23)	1·13
C(5)—C(6)	1·50	C(14)-C(8)	1·46	O(22)-C(21)	1·52
C(6)—C(7)	1·54	C(8)—C(15)	1·42	C(3)—O(24)	1·21
C(7)—C(8)	1·58	C(15)-C(16)	1·56	C(2)—Br	1·955

Bond angles

10—1—2	114	10—5—6	112	12-13-14	105
1—2—3	113	5—6—7	112	13-14—8	104
2—3—4	115	6—7—8	116	12-13-16	113
3—4—5	102	7—8—9	103	16-13-14	103
4—5-10	116	8—9-10	123	14—8-15	100
5-10—1	105	9-10—5	108	8-15-16	112
1—2-Br	113	5-10-20	110	15-16-13	96
3—2-Br	110	9-10-20	115	15-16-17	114
2—3-24	129	10—9-11	112	13-16-17	106
4—3-24	116	7—8-15	111	16-17-22	104
3—4-18	113	7—8-14	116	16-17-23	124
5—4-18	117	14—8—9	112	23-17-22	128
4—5—6	112	8—9-11	106	17-22-21	107
1-10—9	110	9-11-12	116		
1-10-20	108	11-12-13	116		

Torsion angles

Ring *A*		Ring *B*		Ring *C*		Ring *D*	
1—2	53	9-10	53	9-11	37	13-14	47
2—3	−57	10—5	−52	9—8	−54	14—8	−49
3—4	57	5—6	56	8-14	74	8-15	32
4—5	−61	6—7	−56	14-13	−72	15-16	−4
5-10	60	7—8	47	13-12	59	16-13	−25
10—1	−52	8—9	−49	11-12	−43		

Conformational parameters for the five-membered ring. $\Delta = -45°$, $\varphi_m = 51°$ (Altona, Geise & Romers, 1968).

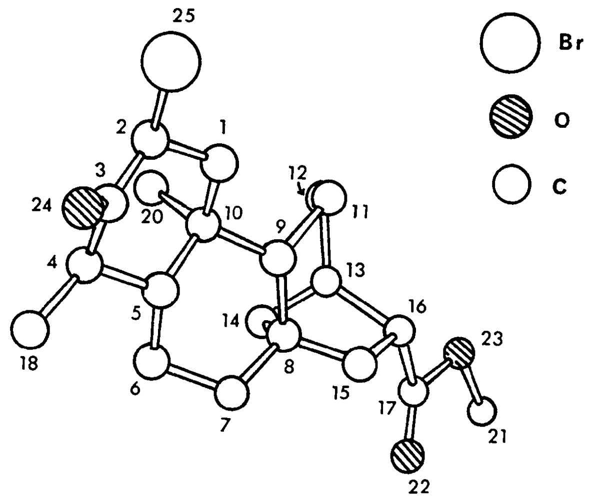

Fig. 2. Molecular structure of methyl 4*R*-2β-bromo-3-oxo-19-nor-16α-(−)-kauran-17-oate and the numbering scheme used in all tables.

however, such interactions are minimal owing to the adjustment of bond and torsion angles. The intramolecular distances for these interactions are 3·38 and 3·40 Å, respectively.

The poor quality of the data leads to a considerable variation in C–C distances and bond angles. The C–C distances in the *A* and *B* rings average 1·54 Å with an average deviation of 0·03 Å while those of the *C* ring average 1·51 Å with an average deviation of 0·05 Å. The distances around the five-membered ring average 1·50 Å with an average deviation of 0·08 Å. The side chain at C(16) shows considerable thermal motion with *B* values ranging from 7·4 for C(17) to 11 for C(21).

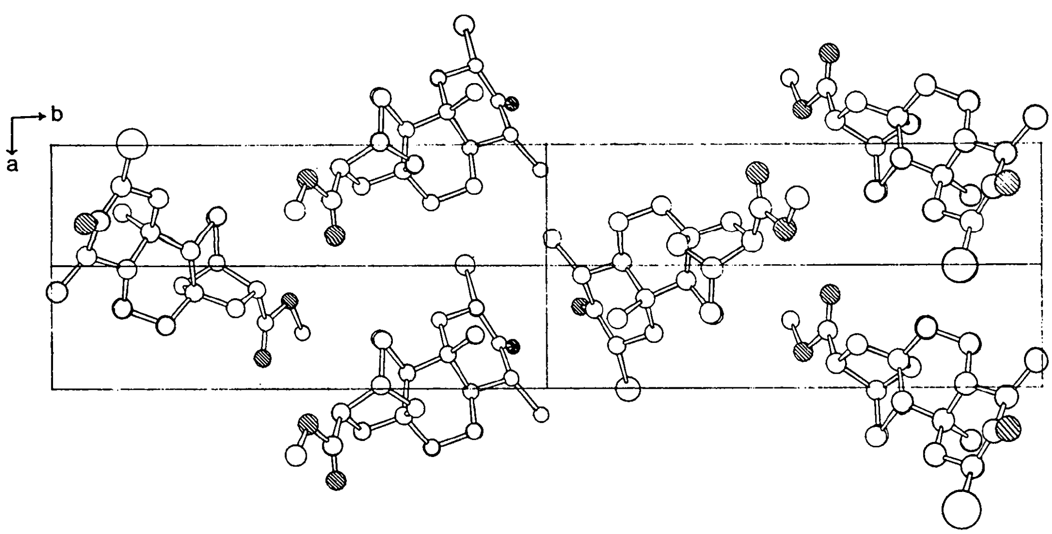

Fig. 1. Projection of the unit-cell contents onto the *ab* plane.

We would like to express our appreciation to the Robert A. Welch Foundation for their financial support (Grant P-074) and to the TCU Research Foundation for the equipment.

References

ALTONA, A. C., GEISE, H. J. & ROMERS, C. (1968). *Tetrahedron*, **24**, 13–29.
CROMER, D. T. & WABER, J. T. (1965). *Acta Cryst.* **18**, 104–109.
GOODWIN, T. W. (1971). *Aspects of Terpenoid Chemistry and Biochemistry, Proceedings of The Phytochemical Society Symposium*, Liverpool, April 1970. London: Academic Press.
HANSON, J. R. (1968). *The Tetracyclic Diterpenes*. Oxford: Pergamon Press.
HANSON, J. R., MCLAUGHLIN, G. M. & SIM, G. A. (1972). *J. Chem. Soc.* pp. 1124–1130.
KARLE, I. L. (1972). *Acta Cryst.* B**28**, 585–589.
STEWART, R. F., DAVIDSON, E. R. & SIMPSON, W. T. (1965). *J. Chem. Phys.* **42**, 3175–3187.

Acta Cryst. (1976). B**32**, 257

The Crystal and Molecular Structure of Polymeric μ-Dichloro-imidazolocadmium (II)

BY L. R. NASSIMBENI AND A. L. RODGERS
Department of Physical Chemistry, University of Cape Town, South Africa

(*Received* 28 *May* 1975; *accepted* 2 *June* 1975)

The structure of $(CdCl_2.ImH)_\infty$ has been determined from single-crystal X-ray diffraction data collected on a four-circle diffractometer. The analysis was carried out with 655 unique reflexions and refined by full-matrix least-squares calculations to a final R of 0·024. The crystals are orthorhombic, space group $Pbn2_1$ with $a=15·305(5)$, $b=11·102(5)$, $c=3·838(5)$ Å, $Z=4$. The structure is polymeric. The Cd atoms are linked into infinite chains by double Cl bridges. Two such chains running parallel to each other are themselves linked *via* Cd–Cl bonds resulting in a cage-like structure. Each Cd is octahedrally coordinated to five Cl and one N. A trifurcated N–H···Cl interaction is postulated.

Introduction

A study of metal ion–imidazole complexes has been undertaken in view of the important role that imidazole plays in providing potential metal binding sites in proteins. Cd itself has recently gained prominence as a pollutant (Shaikh & Lucis, 1971) and is known to be present in the protein metallothionein (Kagi & Vallee, 1960). The unlikely stoichiometry of the complex which we synthesized, $CdCl_2(Im)$, made a structural determination desirable.

Experimental

The complex was prepared by mixing a saturated solution of cadmium lactate with a 1*M* solution of imidazole prepared in 5*M* hydrochloric acid. The *p*H of the initial lactate solution was 5·9 while that of the imidazole was 6·0. The final *p*H of the mixture was 5·05. The percentage composition was: found: C 14·7, H 1·7, N 11·3, Cd 44·9, Cl 26·9%; calculated for $CdCl_2.ImH$: C 14·33, H 1·60, N 11·14, Cd 44·71, Cl 28·20. The density was determined by flotation in a mixture of *m*-xylene and CH_2I_2. The crystals were white thin, plate-like needles. A single crystal (0·20 × 0·25 × 0·28 mm) was used. The lattice constants (Table 1) were obtained from a least-squares analysis of the settings of 25 reflexions measured on a four-circle diffractometer with Mo $K\alpha$ radiation.

Table 1. *Crystal data*

$C_3H_4N_2.CdCl_2$	
M	= 251·38
Space group:	$Pbn2_1$ (No. 33, C_{2v}^9)
a	= 15·305 (5) Å
b	= 11·102 (5)
c	= 3·838 (5)
V	= 652·14 Å³
D_m	= 2·50 g cm⁻³
D_c	= 2·56 g cm⁻³ for $Z=4$
μ	= 39·27 cm⁻¹
$F(000)$	= 472

The intensities were collected on a Philips PW1100 computer-controlled four-circle diffractometer operating in the ω–2θ scan mode (scan width = 1·00° θ, scan speed = 0·04° θ s⁻¹). With graphite-monochromated Mo $K\alpha$ radiation ($\lambda=0·7107$ Å), 698 reflexions up to $2\theta=50°$ were measured. With the criterion $I_{rel}>2\sigma(I_{rel})$ for an observed reflexion, 43 reflexions were omitted as unobserved leaving 655 unique reflexions which were employed in the structural analysis. Three reference reflexions were measured after every 68 reflexions to monitor stability of operation and crystal decomposi-